Inorganica Chimica Acta 435 (2015) 274–282

Contents lists available at ScienceDirect

Inorganica Chimica Acta

journal homepage: www.elsevier.com/locate/ica

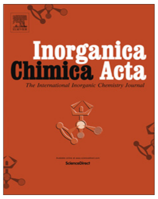

A family of nickel–lanthanide heterometallic dinuclear complexes derived from a chiral Schiff-base ligand exhibiting single-molecule magnet behaviors

He-Rui Wen [a,*], Sui-Jun Liu [a], Xin-Rong Xie [a], Jun Bao [a], Cai-Ming Liu [b,*], Jing-Lin Chen [a]

[a] *School of Metallurgical and Chemical Engineering, Jiangxi University of Science and Technology, Ganzhou 341000, China*
[b] *Beijing National Laboratory for Molecular Sciences, Center for Molecular Science, Institute of Chemistry, Chinese Academy of Sciences, Beijing 100190, China*

ARTICLE INFO

Article history:
Received 10 April 2015
Received in revised form 17 June 2015
Accepted 10 July 2015
Available online 18 July 2015

Keywords:
Nickel–lanthanide
Heterometallic complexes
Chiral Schiff-base
Magnetic properties
Single-molecule magnets

ABSTRACT

A new family of nickel–lanthanide heterometallic dinuclear complexes derived from a chiral Schiff-base ligand, (*R*,*R*)-*N*,*N*′-bis(3-methoxysalicylidene)cyclohexane-1,2-diamine (H_2L), namely $[Ni(L)Ln(NO_3)_3(H_2O)]$ (Ln = Ce (**1**), Nd (**2**)) and $[Ni(L)Ln(NO_3)_3]$ (Ln = Sm (**3**), Eu (**4**), Gd (**5**), Tb (**6**), Dy (**7**) and Yb (**8**)) have been synthesized and structurally characterized. X-ray single-crystal structure determination revealed that these complexes are diphenoxo-bridged Ni^{II}–Ln^{III} dinuclear clusters, which crystallize in the chiral space group $P1$. The solid circular dichroism (CD) spectra confirmed the optical activity and enantiomorphous properties of all these complexes. Magnetic investigations suggested that crystal-field effects and/or the possible antiferromagnetic dipole–dipole interaction between the molecules exist in the complexes and single-ion properties of Ln^{III} ions lead to their magnetic behaviors. The alternating current (ac) magnetic susceptibilities showed that complexes **6** and **7** exhibit field-induced single-molecule magnet behaviors due to the strong anisotropy and important crystal-field effect of the Tb^{III} or Dy^{III} ions. It is noteworthy that the quantum tunneling effect at low temperatures can be effectively suppressed by employing a 2 kOe direct current field.

1. Introduction

The construction of molecule-based magnetic materials has been an active field in chemistry and materials science [1], especially after the discovery of single-molecule magnets (SMMs) in 1993 [2]. The SMMs have attracted much attention over the two decades mainly due to their potential applications in the high-density information storage at the molecular level or nanoscale [3]. However, there are two main issues for the realization of the SMM-based storage technology: (1) the slow magnetic relaxation of the SMMs is currently only accessible below liquid N_2 temperature, thus the magnetic blocking temperature needs to rise significantly; (2) the manufacturing of storage devices encounters great difficulties due to the individual molecules of the SMMs are hard to deposit and address on surfaces [4]. One of the grand challenges in researching for the molecule-based magnets is still, therefore, to design and synthesize the efficient SMMs.

Recently, the lanthanide ions with unique electronic structures have attracted considerable attention because of their unrivaled single-ion anisotropies. The most notable heavy lanthanide ions, such as Dy^{III} [5], Tb^{III} [6], Ho^{III} [7] and Er^{III} [8], have been widely used as the magnetic centers to construct the SMMs [9]. Two strict prerequisites for a molecule as the SMM are that the electronic ground state must be bistable, and the magnetic anisotropy must be present. For the lanthanide ions, other than the ground electronic states of $^1S_0$ and $^8S_{7/2}$, the orbital contribution to the magnetic moment is large and unquenched, and the ligand-field effects in the lanthanide complexes can be regarded as a small-but-significant perturbation [10]. Therefore, the Ln-containing complexes can be considered as the SMMs more likely because of their large angular momentum in the ground electronic states and a large magnetic anisotropies [4]. And more significantly, the lanthanide-based SMMs have already shown considerable potentials to deposit on the surface for device manufacturing [11,4c]. The mononuclear lanthanide compound exhibiting slow relaxation of the magnetization could be called “single-ion magnets” (SIMs) due to the single-ion features [12], while the lanthanide-based SMMs usually include two or more lanthanide ions [4,13].

---

* Corresponding authors. Tel.: +86 797 8312553.
E-mail addresses: wenherui63@163.com (H.-R. Wen), cmliu@iccas.ac.cn (C.-M. Liu).

http://dx.doi.org/10.1016/j.ica.2015.07.009
0020-1693/© 2015 Published by Elsevier B.V.

Since the first ferromagnetic Cu^{II}–Gd^{III} compound was reported by Gatteschi group [14], the 3*d*–4*f* heterometallic complexes have attracted a great deal of interests because they are efficient model compounds in understanding the magnetic exchange between the 3*d* and 4*f* metal ions, and especially, some of 3*d*–4*f* clusters behave as the SMMs [15]. The strong magnetic interaction between the 3*d* and 4*f* ions make it more easier to show the SMM behaviors. The 3*d* metal ions mainly include the Cu^{II} [16], Ni^{II} [17], Co^{II} [18], and Mn^{III} ion [19], and the polydentate Schiff-base ligands are often chose to construct the 3*d*–4*f* heterometallic SMMs [20]. Previous studies revealed that the symmetry of the ligand field around the lanthanide ion strongly affects the magnetic anisotropy [21]. When the chiral ligands are introduced into the magnetic complex, not only the chiral magnets may be obtained, but also the chiral asymmetric coordination environment around the metallic ions can affect the magnetic properties [22,23,4b]. In order to further study the effect of different ligands on the magnetic properties, the chiral hexadentate Schiff-base ligand (Scheme 1) was applied for the synthesis of target SMMs. Herein, we describe the syntheses, crystal structures, and magnetic properties of a new family of 3*d*–4*f* heterometallic dinuclear complexes, namely $[Ni(L)Ln(NO_3)_3(H_2O)]$ (Ln = Ce (**1**), Nd (**2**)) and $[Ni(L)Ln(NO_3)_3]$ (Ln = Sm (**3**), Eu (**4**), Gd (**5**), Tb (**6**), Dy (**7**) and Yb (**8**)) (H_2L = (*R*,*R*)-*N*,*N′*-bis(3-methoxysalicylidene)cyclohexane-1,2-diamine (H_2L)). Remarkably, the Ni^{II}–Tb^{III} (**6**) and Ni^{II}–Dy^{III} (**7**) complexes display field-induced slow magnetic relaxation.

2. Experimental

2.1. General methods

All the reagents and solvents were purchased from the commercial sources and used as received. (*R*,*R*)-1,2-diaminocyclohexane and 3-methoxysalicylaldehyde were purchased form the Aldrich Chemical Co., Inc. The rare earth metal salts $Ln(NO_3)_3·6H_2O$ were prepared from the high purity Ln_2O_3 (99.99%, Ln = Ce, Nd, Sm, Eu, Gd, Tb, Dy and Yb). Elemental analyses for C, H, and N were carried out on a Perkin-Elmer 240C analyzer for complexes. Infrared spectra were recorded on a Vector 22 Bruker spectrophotometer with KBr pellets in the region 400–4000 cm^{-1}. The circular dichroism spectra were recorded on a JASCO J-1500 spectropolarimeter with KBr pellets. Single crystal data were collected on Bruker Apex-II Smart CCD diffractometer using monochromated Mo Kα radiation. The PXRD spectra were recorded on an Empyrean (PANalytical B.V.) diffractometer for a Cu-target tube and a graphite monochromator. Simulation of the PXRD spectra were carried out by the single-crystal data and diffraction-crystal module of the Mercury (Hg) program available free of charge via the Internet at http://www.iucr.org. Variable-temperature magnetic susceptibility, zero-field alternating current (AC) magnetic susceptibility, and field dependence of magnetization were measured on a Quantum Design MPMS XL-5 (SQUID) magnetometer. Diamagnetic corrections were estimated from Pascal's constants for all constituent atoms. The AC susceptibility measurements were carried out in a 2.5 Oe AC field oscillating at 10–1000 Hz, under a 0.1 T static field. To avoid torqueing of the crystallites in the presence of the magnetic field, the samples were crushed before measurements.

2.2. Syntheses of $[Ni(L)]·H_2O$

The chiral Schiff-base ligand (*R*,*R*)-H_2L or (*S*,*S*)-H_2L (H_2L = *N*,*N′*-bis(3-methoxysalicylidene)cyclohexane-1,2-diamine) was synthesized by the condensation of (*R*,*R*)-1,2-diaminocyclohexane or (*S*,*S*)-1,2-diaminocyclohexane with 3-methoxysalicylaldehyde in methanol and directly used without further separation. A methanolic solution (10 mL) of $Ni(CH_3COO)_2·4H_2O$ (2 mmol) was added to a methanolic solution (50 mL) containing the Schiff-base (*R*,*R*)-H_2L or (*S*,*S*)-H_2L (2 mmol), and the reaction mixture was stirred for 2 h at room temperature. The solvents were removed under vacuo and the resulting orange-yellow solid was washed two times with acetone. The orange-yellow needle-shaped crystals were obtained by recrystallization in acetonitrile. Single crystal measurements showed that the $[Ni(L)]·H_2O$ is a mononuclear Ni^{II} complex crystallized in the chiral space group $P2_12_12_1$ (Fig. S1, SI).

2.3. Syntheses of $[Ni(L)Ln(NO_3)_3(H_2O)_x]$ (**1**–**8**, Ln = Ce, Nd, Sm, Eu, Gd, Tb, Dy, Yb)

A acetonitrile solution (10 mL) of $Ln(NO_3)_3·6H_2O$ (0.1 mmol) was added to $[Ni(L)]·H_2O$ (0.1 mmol) in acetonitrile (10 mL), after

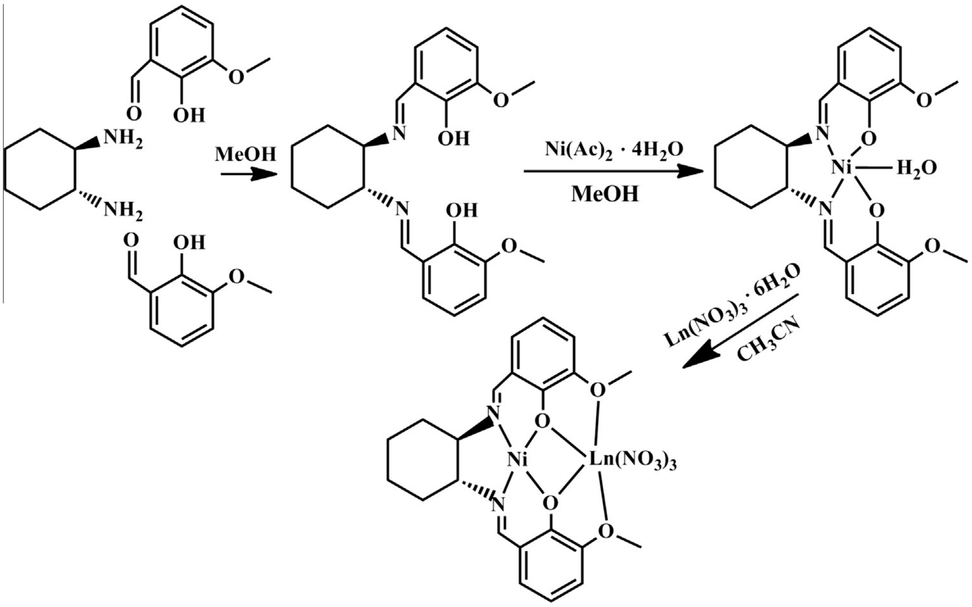

Scheme 1. The synthetic route of the complexes.

stirred for 12 h at room temperature, the reaction mixture was heated to 60 °C and continued to stir for 30 min, an orange-red solution was obtained and then filtered. The red block-shaped crystals were obtained after slow evaporation of the resulting filtrate under 60 °C in a constant temperature oven for 24 h. Yields: 50–60%. Observed/calculated elemental analyses and selected IR spectra data of **1**–**8** are listed in Table S1 (SI). The enantiomers of complexes **1**–**8**, $[Ni((S,S)\text{-}L)Ln(NO_3)_3]_2$, were synthesized by the same procedure except that (*R*,*R*)-H_2L was replaced by (*S*,*S*)-H_2L.

2.4. X-ray crystallography

The crystal structures of complexes **1**–**8** were determined on a Bruker Apex-II Smart CCD diffractometer using monochromated Mo Kα radiation ($\lambda = 0.71073$ Å). The data were collected at room temperature. Absorption corrections were applied using SADABS supplied by Bruker. Structures were solved by direct methods using the program SHELXTL-97. The positions of the metal atoms and their first coordination spheres were located from direct-methods *E*-maps; other non-hydrogen atoms were found using alternating difference Fourier syntheses and least squares refinement cycles, and during the final cycles, were refined anisotropically. Hydrogen atoms were placed in calculated position and refined as riding atoms with a uniform value of U_{iso} [24]. The hydrogen atoms of the water molecules in **1** and **2** were located from Fourier difference maps with suitable restraint. During the refinement process, the DELU and EADP commands were used to make the bonds and temperature factors more reasonable. It should be mentioned

Table 1
Crystal data and refinement for the complexes **1**–**4**.

Complex	R–Ni–Ce (**1**)	R–Ni–Nd (**2**)	R–Ni–Sm (**3**)	R–Ni–Eu (**4**)
Formula	$C_{22}H_{26}O_{14}N_5NiCe$	$C_{22}H_{26}O_{14}N_5NiNd$	$C_{22}H_{24}O_{13}N_5NiSm$	$C_{22}H_{24}O_{13}N_5NiEu$
Formula weight	783.31	787.43	775.52	777.13
T (K)	298(2)	293(2)	293(2)	293(2)
Crystal system	triclinic	triclinic	triclinic	triclinic
Space group	*P*1	*P*1	*P*1	*P*1
a (Å)	7.8582(8)	7.8198(4)	9.3450(5)	9.3421(5)
b (Å)	12.6490(13)	12.6563(6)	12.1708(6)	12.1826(6)
c (Å)	14.1306(15)	14.1463(6)	12.2478(6)	12.2389(7)
α (°)	92.809(7)	93.125(3)	78.1000(10)	77.953(2)
β (°)	91.593(7)	91.562(4)	83.6770(10)	83.572(2)
γ (°)	100.324(6)	100.449(3)	89.7630(10)	89.860(2)
V ($Å^3$)	1379.2(2)	1373.81(11)	1354.54(12)	1353.37(13)
Z	2	2	2	2
D_{calc} (Mg/m^3)	1.886	1.904	1.917	1.907
μ (mm^{-1})	2.392	2.634	2.917	3.068
F(000)	782	786	770	772
Flack parameter	0.055(5)	0.12(4)	0.106(14)	−0.030(12)
R_{int}	0.1250	0.0412	0.0270	0.0413
Goodness-of-fit (GOF)	1.005	0.990	1.025	1.010
Final R_1[a]	0.0996	0.0659	0.0297	0.0284
wR_2[b] [$I > 2\sigma(I)$]	0.2553	0.1733	0.0592	0.0488
R_1, wR_2 (all data)	0.1654, 0.2984	0.1051, 0.1685	0.0408, 0.0635	0.0432, 0.0525

[a] $R_1 = \sum||F_o| - |F_c||/\sum|F_o|$.
[b] $wR_2 = [\sum[w(F_o^2 - F_c^2)^2]/\sum w(F_o^2)^2]^{1/2}$.

Table 2
Crystal data and refinement for the complexes **5**–**8**.

Complex	R–Ni–Gd (**5**)	R–Ni–Tb (**6**)	R–Ni–Dy (**7**)	R–Ni–Yb (**8**)
Formula	$C_{22}H_{24}O_{13}N_5NiGd$	$C_{22}H_{24}O_{13}N_5NiTb$	$C_{22}H_{24}O_{13}N_5NiDy$	$C_{22}H_{24}O_{13}N_5NiYb$
Formula weight	782.42	784.09	787.67	798.21
T (K)	293(2)	296(2)	296(2)	295(2)
Crystal system	Triclinic	Triclinic	Triclinic	Triclinic
Space group	*P*1	*P*1	*P*1	*P*1
a (Å)	9.3445(9)	9.3289(2)	9.3464(7)	9.3385(3)
b (Å)	12.1922(11)	12.1567(2)	12.1439(9)	12.1287(4)
c (Å)	12.2498(11)	12.2318(2)	12.2489(10)	12.2211(4)
α(°)	77.962(3)	102.004 (1)	101.885(6)	102.0320(10)
β (°)	83.604(3)	96.420 (1)	96.406(5)	96.3240(10)
γ (°)	89.986(3)	90.017 (1)	90.136(5)	90.3200(10)
V ($Å^3$)	1356.1(2)	1347.95 (4)	1351.51(18)	1344.98(8)
Z	2	2	2	2
D_{calc} (Mg/m^3)	1.916	1.932	1.936	1.971
μ (mm^{-1})	3.194	3.377	3.516	4.232
F(000)	774	776	778	786
Flack parameter	−0.025(14)	0.057(15)	0.17(3)	0.065(14)
R_{int}	0.0304	0.0484	0.0742	0.0262
Goodness-of-fit (GOF)	1.045	1.017	0.986	1.042
Final R_1[a]	0.0266	0.0327	0.0779	0.0298
wR_2[b] [$I > 2\sigma(I)$]	0.0466	0.0566	0.1800	0.0608
R_1, wR_2 (all data)	0.0379, 0.0499	0.0530, 0.0619	0.1143, 0.2056	0.0419, 0.0657

[a] $R_1 = \sum||F_o| - |F_c||/\sum|F_o|$.
[b] $wR_2 = [\sum[w(F_o^2 - F_c^2)^2]/\sum w(F_o^2)^2]^{1/2}$.

that the space groups of all the complexes are $P1$ but not $P\bar{1}$, which is consistent with the fact that the complexes derived from chiral ligands usually crystallize in chiral space groups, and is also consistent with the chair conformation of cyclohexyl and the CD spectra. A summary of the crystal data collection and refinement parameters is given in Tables 1 and 2.

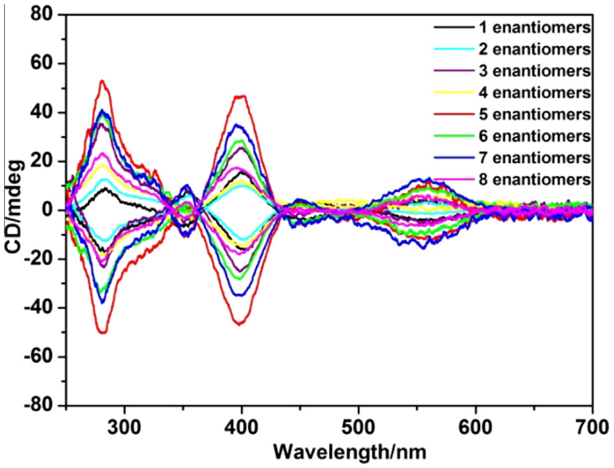

Fig. 1. Circular dichroism spectra of complexes **1**–**8** and their enantiomers in KBr pellets.

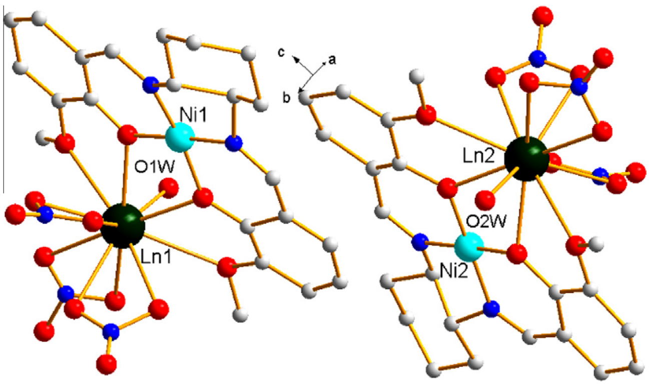

Fig. 2. View of the molecular structure for $[Ni(L)Ln(NO_3)_3(H_2O)]$ (Ln = Ce (**1**) and Nd (**2**)) (the hydrogen atoms omitted for clarity).

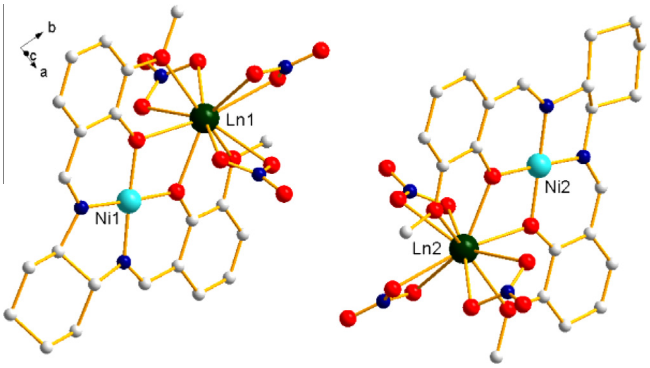

Fig. 3. View of the molecular structure for $[Ni(L)Ln(NO_3)_3]$ (Ln = Sm (**3**), Eu (**4**), Gd (**5**), Tb (**6**), Dy (**7**), Yb (**8**)) (the hydrogen atoms omitted for clarity).

3. Results and discussion

3.1. Synthesis, IR and CD Spectra

All complexes were synthesized through the reactions between $[Ni(L)]\cdot H_2O$ and $Ln(NO_3)_3\cdot 6H_2O$ in anhydrous acetonitrile. The resulting products are largely dependent on the environmental temperature. If we let the resulting filtrate to evaporate slowly at room temperature, no crystalline materials could be obtained. However, when the resulting filtrate was placed in a constant temperature oven to evaporate fairly fast at above room temperature, the reaction was able to get crystals of target complexes. The selected IR spectra data and elemental analyses for complexes **1**–**8** are listed in Table S1 (SI). The characteristic —C=N— stretching of $[Ni(L)]\cdot H_2O$ appears as a strong band at 1619 cm^{-1}, while this vibration in the eight Ni^{II}–Ln^{III} complexes is also observed as a strong signal, but in the range 1623–1628 cm^{-1}. The presence of nitrates in the Ni^{II}–Ln^{III} complexes is evidenced by two strong signals at about 1475 and 1315 cm^{-1}. Two medium intensity bands at 3588 and 3537 cm^{-1} for $[Ni(L)]\cdot H_2O$ are indicative that the water molecule exists in the complex. The structure composition of the Ni^{II}–Ce^{III} (**1**) and Ni^{II}–Nd^{III} (**2**) is $[Ni(L)Ln(NO_3)_3(H_2O)]$ (Ln = Ce, Nd), and its IR spectra exhibit one band of medium intensity at 3250 cm^{-1}, which can be assigned to the water molecule stretching, and the elemental analyses of the compounds are also matched with a composition containing one H_2O molecule. The structure composition of the other six Ni^{II}–Ln^{III} compounds is

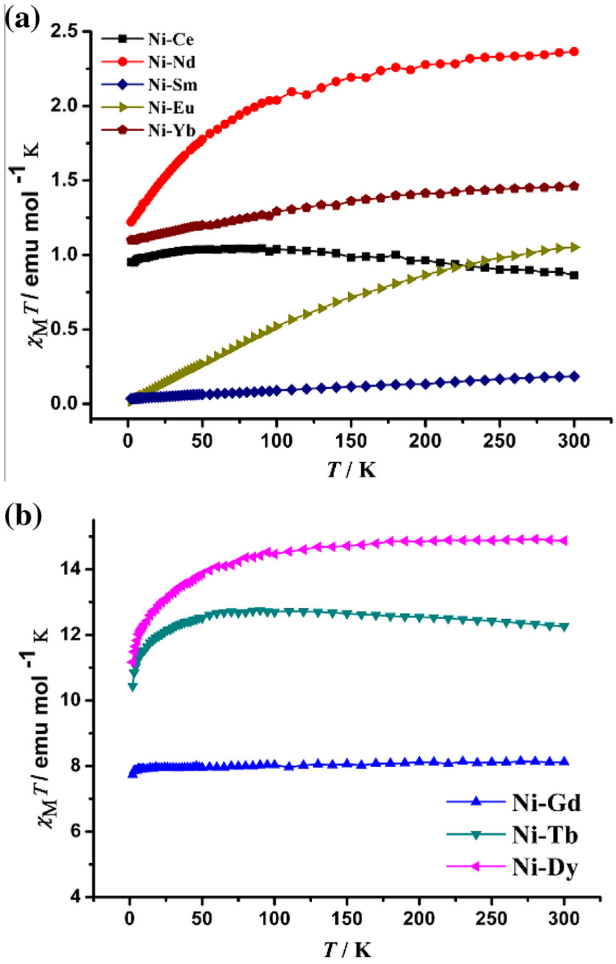

Fig. 4. Temperature dependence of magnetic susceptibilities in the forms of $\chi_M T$ for **1**–**8**.

[Ni(L)Ln(NO_3)$_3$] (Ln = Sm, Eu, Gd, Tb, Dy and Yb), and their IR spectra and elemental analyses are well matched with the molecular composition.

In order to confirm the optical activity and enantiomeric nature, the solid circular dichroism (CD) spectra in KBr pellets for complexes **1**–**8** were measured. For *R* enantiomers of **1**–**8**, the CD spectra exhibit strong negative Cotton effect around 280 and 400 nm, and a weak positive dichroic signal centered at 558 nm, while the *S* enantiomers show Cotton effects of the opposite signals at the same wavelengths (Fig. 1). The two CD peaks can be assigned to the charge-transfer of the UV–Vis absorption spectra of these complexes and the d-d transitions of Ni(II). The CD spectra of the enantiomers further confirmed the optical activity and enantiomorphous properties.

3.2. Crystal structure descriptions

The structures of these complexes were measured by the X-ray single-crystal diffractometer, which revealed that all complexes are neutral diphenoxo-bridged Ni^{II}–Ln^{III} dinuclear clusters with the chiral space group *P*1. However, they exhibit two different structures: the one possesses one coordinated water (**1** and **2**), while the other has no coordinated water (**3**–**8**). There are two crystallography independent molecules in the crystal cell (Figs. 2 and 3). In each cluster, the inner N_2O_2 donors of the Schiff-base ligand are bonded to the Ni^{II} ion (Fig. S1), while the Ln^{III} ion is coordinated by two bridging phenoxo O atoms and two O atoms from two methoxy groups of this Schiff-base ligand, and six O atoms from three chelating nitrates. For **1** and **2**, the Ln^{III} ion is also coordinated by an additional O atom from the coordinated hydrate molecule. The Ni–N/O bond lengths lie in the range 1.74(2)–1.941(15) Å, which are consistent with those of the other Schiff-base Ni^{II} complexes showing the square coordination geometry [17d]. The Ni^{II}, Ln^{III} ions and two bridging phenoxo O atoms are not on a plane but with a dihedral angle between the NiO1O2 and LnO1O2 planes being equal to 1.31–7.55°, and the dihedral angle deviation gradually decrease from the light to heavy lanthanides. From Ni^{II}–Ce^{III} to Ni^{II}–Yb^{III}, the Ln–O(phenoxo), Ln–O(methoxy) and Ln–O(nitrate) bond lengths decrease owing to the lanthanide contraction effect, for examples, the Ce–O(phenoxo), Ce–O(methoxy) and Ce–O(nitrate) bond lengths are 2.447(15)–2.596(16), 2.789(19)–2.87(2) and 2.476(16)–2.720(16) Å, respectively, while the Yb–O(phenoxo), Yb–O(methoxy) and Yb–O(nitrate) bond lengths are 2.281(10)–2.329(10), 2.476(11)–2.529(10), and 2.357(6)–2.595(6) Å, respectively. The Ln–O(phenoxo) bond lengths are shorter than the corresponding Ln–O(methoxy) and Ln–O(nitrate) bond distances, and the intramolecule Ni$^{II}\cdots$Ln^{III} separation (Ni1$\cdots$Ln1) decreases from 3.4635(39) in the Ni^{II}–Ce^{III} to 3.3456(19) Å in the Ni^{II}–Yb^{III}. The selected bond lengths and angles for complexes **1**–**8** are listed in Tables S2–S9 (SI).

Usually the Ni^{II} ion assumes square or octahedral coordination geometry. In these Ni^{II}–Ln^{III} dinuclear complexes, the Ni^{II} ion is tetra-coordinated by the two imine N atoms and two bridging phenoxo O atoms of the Schiff-base ligand, and thus adopts an

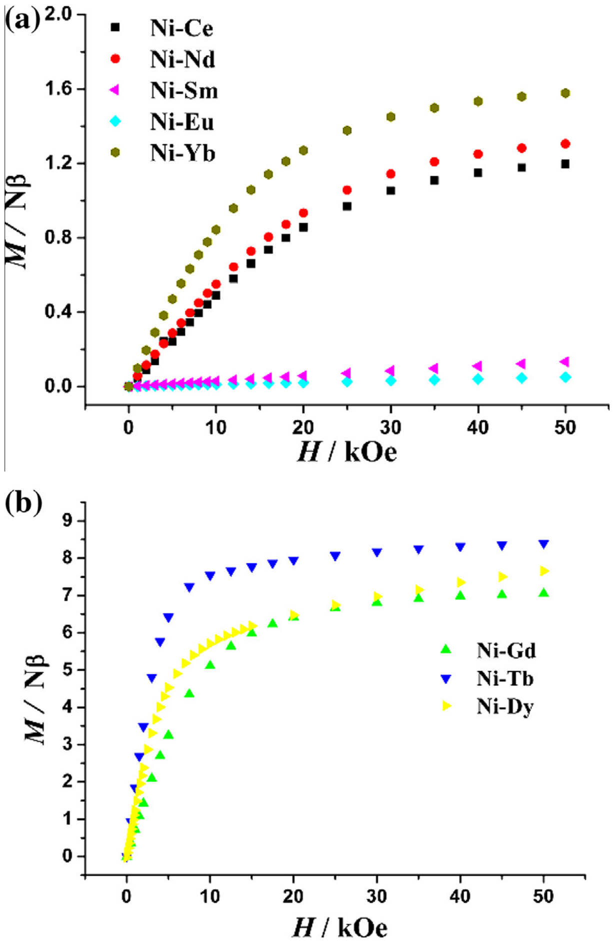

Fig. 5. Field dependence of the magnetizations of **1**–**8** measured at 2 K.

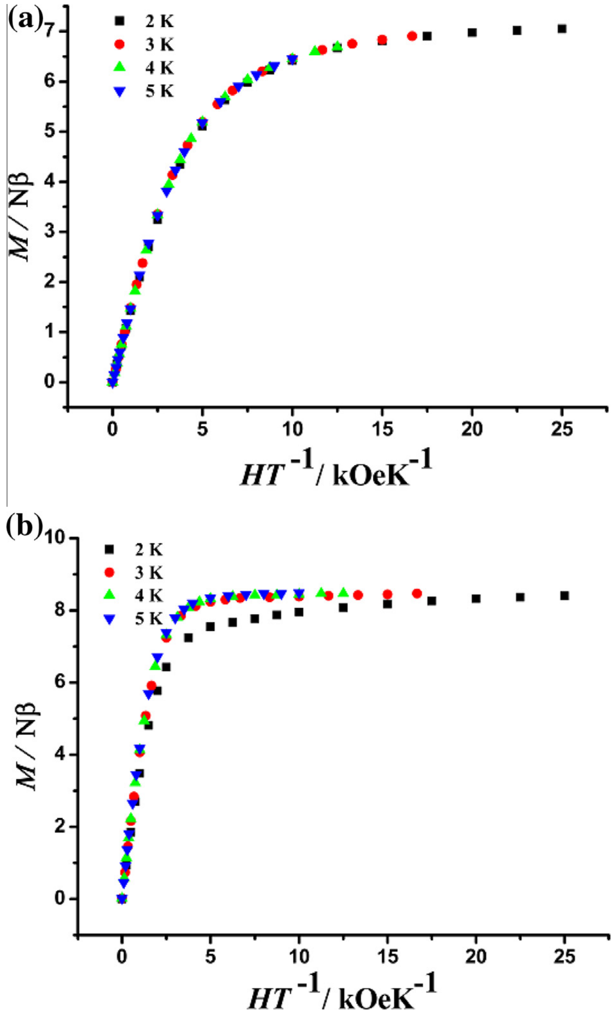

Fig. 6. The plots of *M* versus *H*/*T* for **5** (a) and **6** (b) in the field range 0–50 kOe.

approximate square coordination environment, while the Ln^{III} centers exhibit two kinds of coordination environments. The Ce^{III} in **1** is eleven-coordinated with two bridging phenoxo O atoms, two methoxy O atoms, six O atoms of three chelating nitrates and one water O atom (Fig. 2). While the Sm^{III} in **3** is ten-coordinated with two bridging phenoxo O atoms, two methoxy O atoms, and six O atoms of three chelating nitrates (Fig. 3). In the light lanthanide complexes Ni^{II}–Ce^{III} (**1**) and Ni^{II}–Nd^{III} (**2**), the Ln^{III} centers are eleven-coordinated because of the additional coordination by a water molecule, while in the heavier lanthanides complexes, Ni^{II}–Sm^{III} (**3**), Ni^{II}–Eu^{III} (**4**), Ni^{II}–Gd^{III} (**5**), Ni^{II}–Tb^{III} (**6**), Ni^{II}–Dy^{III} (**7**), and Ni^{II}–Yb^{III} (**8**), the Ln^{III} centers are ten-coordinated duo to absence of coordination water molecule. The coordination number of the Ln^{III} ion decreases in the heavier lanthanides complexes mainly due to the lanthanide contraction.

3.3. Magnetic properties

Before the magnetic measurements, the X-ray powder diffraction (PXRD) measurements of the crushed crystalline samples of **1**–**8** were carried out to confirm their phase purities (Fig. S2, SI). The magnetic properties of **1**–**8** were investigated by magnetic susceptibility measurements in 2–300 K range at 1 kOe field and the isothermal field-dependent magnetizations $M(H)$ at fields up to 50 kOe at 2 K.

The χ_MT values at 300 K for **1**–**2** and **5**–**8** are 0.86, 2.36, 8.12, 12.26, 14.87 and 1.46 emu mol^{-1} K (Fig. 4), respectively, being basically in agreement with the corresponding spin-only values expected for one Ln^{III} isolated ion (C_{Ce} = 0.80 emu mol^{-1} K, C_{Nd} = 1.64 emu mol^{-1} K, C_{Gd} = 7.88 emu mol^{-1} K, C_{Tb} = 11.82 emu mol^{-1} K, C_{Dy} = 14.17 emu mol^{-1} K and C_{Yb} = 2.57 emu mol^{-1} K), indicating the ground state of the Ni^{II} is low spin (C_{Ni} = 0 emu mol^{-1} K) due to its square coordination geometry, and the susceptibilities of all the Ni^{II}–Ln^{III} complexes arise only due to the Ln^{III} ion. With the temperature decreasing, the χ_MT values stays nearly constant in the high temperature range and decrease quickly at very low temperatures to the minimum values (0.95, 1.22, 7.73, 10.44, 11.17 and 1.10 emu mol^{-1} K, respectively) at 2 K, which is likely due to crystal-field effects (*i.e.* thermal depopulation of the Ln^{III} Stark sublevels) and/or the possible antiferromagnetic dipole–dipole interaction between the molecules. Because of these types of population variation, the χ_MT values should be expected to diminish gradually on steady cooling of the complexes. For **3** and **4**, the χ_MT values are equal to 0.18 and 1.05, emu mol^{-1} K at 300 K, which agrees with the values of one isolated Sm^{III} or Eu^{III} ions (C_{Sm} = 0.28 emu mol^{-1} K, C_{Eu} = 1.36 emu mol^{-1} K) calculated from the Van Vleck equation allowing for population of the lower excited state. With the temperature cooling, the χ_MT decreases continuously as a result of the depopulation of the Stark levels and is close to zero (0.035 and 0.016 emu mol^{-1} K) at 2.0 K, corresponding to a non-magnetic ground state. For Sm^{III} and Eu^{III} complexes, both the possible thermal population of the higher states and crystal field effects have an influence on the magnetic properties of **3** and **4** because of the weak energy separation. Therefore, the magnetic properties of **1**–**8** result from the single-ion behaviors of the Ln^{III} ions.

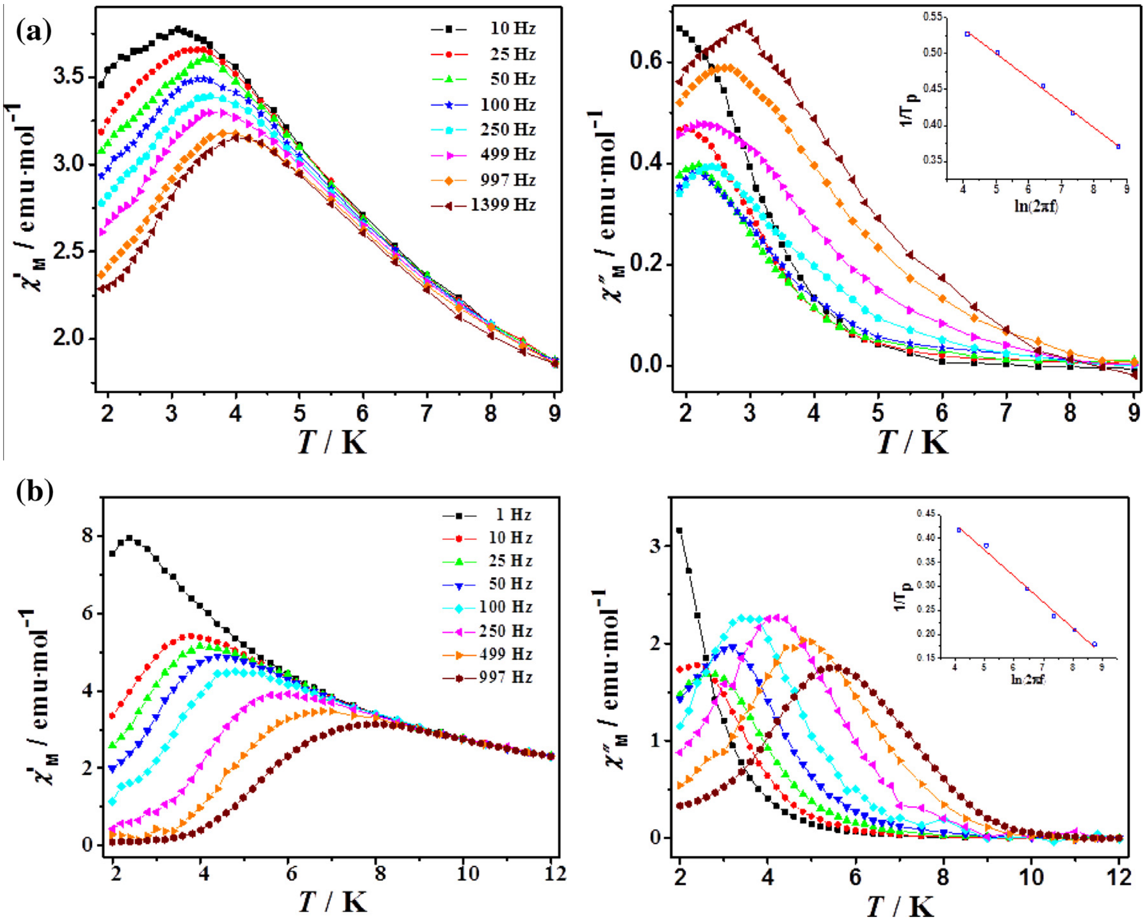

Fig. 7. Temperature dependence of the χ_{ac} at different frequencies with H_{dc} = 2 kOe and H_{ac} = 2.5 Oe and the least-squares fit of the experimental data to the Arrhénius equation for **6** (a) and **7** (b).

The field dependence of the magnetization was recorded at different temperatures. For **1**–**8**, the magnetizations increase quickly at very low field, reaching about 0.49, 0.55, 0.03, 0.01, 5.11, 7.55, 5.71 and 0.84 Nβ at 10 kOe, respectively (Fig. 5). In the high field region the increase of magnetizations is slow and linear, which may be attributed to the anisotropy. At 2 K, the *M* values reach to 1.20, 1.31, 0.13, 0.05, 7.05, 8.40, 7.66 and 1.58 Nβ at 50 kOe, respectively, being smaller than the theoretical saturated values anticipated for one corresponding Ln^{III} ion. This can be explained by the fact that the depopulation of the Stark levels of the Ln^{III} $^{2S+1}L_J$ ground state under the ligand-field perturbation produces a much smaller effective spin [25]. Additionally, the *M* versus *H* plots for **5**–**7** almost do not show any hysteresis at 2 K (Fig. S3, SI) probably due to the super-low blocking temperature. The *M* versus *H*/*T* (Fig. 6a) data of **5** at 2–5 K show nearly overlapping curves, which indicates there is almost no anisotropy in the complex. While, there are non-superposition plots of *M* versus *H*/*T* data and a rapid increase of the magnetizations at low fields for **6** (Fig. 6b), which eventually reaches the maximum value at 50 kOe without any sign of saturation. The reason is most likely because of strong anisotropy and important crystal-field effect of the Tb^{III} ions [26].

In order to further elucidate possible SMM behaviors of **6** and **7**, alternating current (ac) susceptibility measurements were performed in the different temperature ranges under $H_{dc} = 0$ kOe and $H_{ac} = 2.5$ Oe for variable frequencies. No obvious frequency- and temperature-dependent ac signals were observed for **6** and **7**. Therefore, a suitable dc field (2 kOe) was used to suppress the quantum tunneling effect at low temperatures. For **6** and **7**, the curves of the ac magnetic susceptibilities show that both in-phase and out-of-phase signals are frequency- and temperature-dependent with a series of frequency-dependent peaks for the out-of phase ac signals (Fig. 7), these are typical features for the field-induced SMM behaviors. The strong anisotropies may result in the SMM behaviors of **6** and **7** [27]. To obtain the relaxation energy barrier and relaxation time of **6** and **7**, the best fitting based on the Arrhénius law $1/T_p = -k_B/\Delta E[\ln(2\pi f) + \ln(\tau_0)]$ [28] gave the energy barrier of 29.12 K (**6**) and 18.40 K (**7**), and the pre-exponential factor of 3.21×10^{-9} s (**6**) and 7.39×10^{-6} s (**7**) (Fig. 7, inset). The values are in agreement with the observed τ_0 and $\Delta E/k_B$ for the Ln^{III}-based SMMs, and the values of $\Delta E/k_B$ are higher than those of the similar achiral dinuclear Ni–Ln complexes [17f]. Furthermore, at fixed temperatures of 2 and 3 K with a 2 kOe dc field for **6**, the Cole–Cole plots (Fig. 8) from 1 to 1488 Hz in the form of χ''_M versus χ'_M exhibit multiple relaxation processes and such a field-induced multiple relaxation processes was also observed in the other SMMs/SIMs [29]. The existence of two crystallography independent lanthanide ions probably is the main reason for **6** and **7** to exhibit the multiple relaxation processes [30]. As aforementioned, complexes **6** and **7** display the field-induced SMM behaviors. Most of Ni^{II}–Ln^{III} complexes behaving as SMMs contain paramagnetic Ni^{II} ions, however, the Ni^{II}–Ln^{III} system that exhibits the highest energy barrier ever found is a {Ni_3Dy_2} cluster complex [31] in which the Ni^{II} ions, as our compounds, are diamagnetic. Compared with the similar works using achiral Schiff-base ligands [23a], we investigate the ac properties of target complexes in details. Therefore, two field-induced chiral SMMs have been successfully constructed, which open a new way to the synthesis of SMMs in the Ni–Ln system.

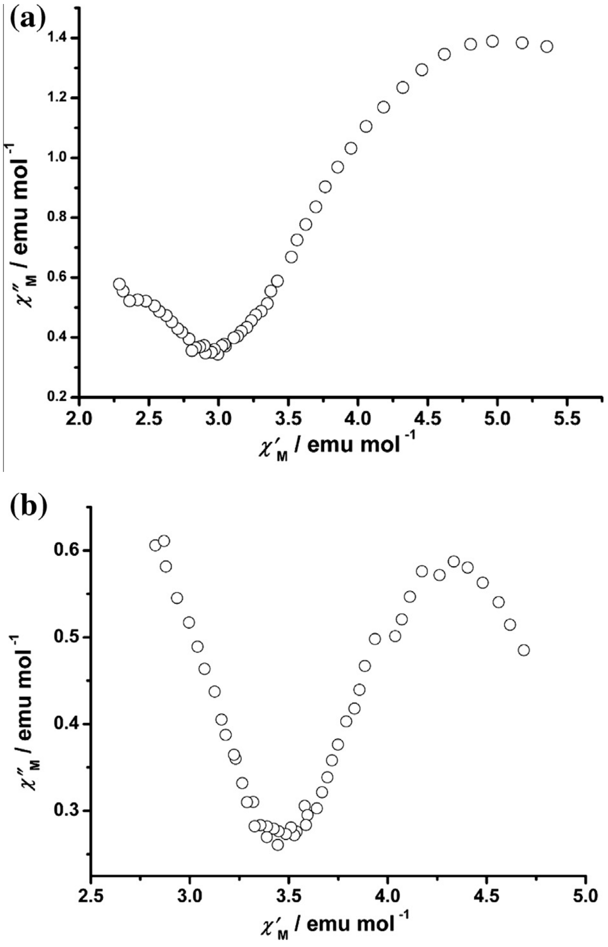

Fig. 8. Cole–Cole plots for complex **6** measured at 2 K (a) and 3 K (b) with 2 kOe dc field.

4. Conclusion

The synthesis, structural characterization and magnetism of a new family of Ni^{II}–Ln^{III} dinuclear complexes derived from a chiral Schiff-base ligand have been studied. Complexes **1**–**8** are neutral diphenoxo-bridged Ni^{II}–Ln^{III} dinuclear compound and crystallize in the same chiral space group *P*1. The solid CD spectra confirm the optical activity and enantiomorphous properties of all these complexes. The magnetic behaviors of **1**–**8** attribute to single-ion properties of the Ln^{III} ions, and crystal-field effects and/or the possible antiferromagnetic dipole–dipole interaction between the molecules have a great influence on their magnetic properties. For **6** and **7**, the ac magnetic susceptibilities show that both χ' and χ'' are strongly frequency- and temperature-dependent under a 2 kOe dc field. These results clearly indicate that complexes **6** and **7** are chiral field-induced SMMs.

Acknowledgments

This work was supported by the National Natural Science Foundation of China (21161008 and 91022014) and the Natural Science Foundation of Jiangxi Province (Grant 20151BAB213003).

Appendix A. Supplementary material

CCDC 1020972–1020975 (complexes **1**–**3** and **7**) and 1043143–1043146 (complexes **4**–**6** and **8**) contain the supplementary crystallographic data for this paper. These data can be obtained free of charge from The Cambridge Crystallographic Data Centre via www.ccdc.cam.ac.uk/data_request/cif. Supplementary data associated with this article can be found, in the online version, at http://dx.doi.org/10.1016/j.ica.2015.07.009.

Reference

[1] (a) O. Kahn, V.C.H. Weinhem, Germany, Molecule Magnetism. 1993.;
(b) K.R. Dunbar, R.A. Heintz, Prog. Inorg. Chem. 45 (1997) 283391;
(c) L.M.C. Beltran, J.R. Long, Acc. Chem. Res. 38 (2005) 325334;
(d) G. Poneti, L. Poggini, M. Mannini, B. Cortigiani, L. Sorace, E. Otero, P. Sainctavit, A. Magnani, R. Sessolia, A. Deia, Chem. Sci. 6 (2015) 22682274;
(e) G. Poneti, M. Mannini, B. Cortigiani, L. Poggini, L. Sorace, E. Otero, P. Sainctavit, R. Sessoli, A. Dei, Inorg. Chem. 52 (2013) (1805) 11798.

[2] (a) R. Sessoli, D. Gatteschi, A. Caneschi, M.A. Novak, Nature 365 (1993) 141;
(b) D. Gatteschi, A. Caneschi, L. Pardi, R. Sessoli, Science 265 (1994) 1054;
(c) D. Gatteschi, R. Sessoli, Angew. Chem., Int. Ed. 42 (2003) 268297;
(d) M. Yamanouchi, D. Chiba, F. Matsukura, H. Ohno, Nature 428 (2004) 539542;
(e) E. Saitoh, H. Miyajima, T. Yamaoka, G. Tatara, Nature 432 (2004) 203206;
(d) E.K. Brechin, Chem. Commun. (2005) 51415153;
(f) M. Evangelisti, F. Luis, L.J. De Jongh, M. Affronte, J. Mater. Chem. 16 (2006) 25342549.

[3] (a) X. Yi, G. Calvez, C. Daiguebonne, O. Guillou, K. Bernot, Inorg. Chem. 54 (2015) 5213;
(b) M. Mannini, F. Pineider, P. Sainctavit, C. Danieli, E. Otero, C. Sciancalepore, A.M. Talarico, M.-A. Arrio, A. Cornia, D. Gatteschi, R. Sessoli, Nat. Mater. 8 (2009) 194–197;
(c) K. Katoh, Y. Yoshida, M. Yamashita, H. Miyasaka, B.K. Breedlove, T. Kajiwara, S. Takaishi, N. Ishikawa, H. Isshiki, Y.F. Zhang, T. Komeda, M. Yamaguchi, J. Takeya, J. Am. Chem. Soc. 131 (2009) 99679976;
(d) K. Bernot, F. Pointillart, P. Rosa, M. Etienne, R. Sessoli, D. Gatteschia, Chem. Commun. 46 (2010) 6458;
(e) M. Mannini, F. Pineider, C. Danieli, F. Totti, L. Sorace, Ph. Sainctavit, M.A. Arrio, E. Otero, L. Joly, J.C. Cezar, A. Cornia, R. Sessoli, Nature 468 (2010) 417.

[4] (a) D.N. Woodruff, R.E.P. Winpenny, R.A. Layfield, Chem. Rev. 113 (2013) 51105148;
(b) R. Sessoli, M.-E. Boulon, A. Caneschi, M. Mannini, L. Poggini, F. Wilhelm, A. Rogalev, Nat. Phys. 11 (2015) 6974;
(c) M. Mannini, F. Bertani, C. Tudisco, L. Malavolti, L. Poggini, K. Misztal, D. Menozzi, A. Motta, E. Otero, P. Ohresser, P. Sainctavit, G.G. Condorelli, E. Dalcanale, R. Sessoli, Nat. Comm. 5 (2014) 4582.

[5] (a) R. Sessoli, A.K. Powell, Coord. Chem. Rev. 253 (2009) 23282341;
(b) L. Sorace, C. Benelli, D. Gatteschi, Chem. Soc. Rev. 40 (2011) 30923104;
(c) P.-E. Car, M. Perfetti, M. Mannini, A. Favre, A. Caneschi, R. Sessoli, Chem. Commun. 47 (2011) 3751;
(d) K. Bernot, J. Luzon, L. Bogani, M. Etienne, C. Sangregorio, M. Shanmugam, A. Caneschi, R. Sessoli, D. Gatteschi, J. Am. Chem. Soc. 131 (2009) 5573;
(e) J. Tang, I. Hewitt, N.T. Madhu, G. Chastanet, W. Wernsdorfer, C.E. Anson, C. Benelli, R. Sessoli, A.K. Powell, Angew. Chem., Int. Ed. 45 (2006) 1729.

[6] (a) N. Ishikawa, J. Phys. Chem. A 103 (2003) 58315835;
(b) T. Kajiwara, K. Takahashi, T. Hiraizumi, S. Takaishi, M. Yamashita, CrystEngComm 11 (2009) 21102116.

[7] N. Ishikawa, M. Sugita, W. Wernsdorfer, J. Am. Chem. Soc. 127 (2005) 36503651.

[8] (a) M.A. AlDamen, J.M. Clemente-Juan, E. Coronado, C. Martí-Gastaldo, A. Gaita-Ariño, J. Am. Chem. Soc. 130 (2008) 8874;
(b) M.A. AlDamen, S. Cardona-Serra, J.M. Clemente-Juan, E. Coronado, A. Gaita-Ariño, C. Martí-Gastaldo, F. Luis, O. Montero, Inorg. Chem. 48 (2009) 3467;
(c) M. Perfetti, G. Cucinotta, M.-E. Boulon, Fadi El Hallak, Song Gao, R. Sessoli, Chem. Eur. J. 20 (2014) 14051;
(d) M.E. Boulon, G. Cucinotta, S.S. Liu, S.D. Jiang, L. Ungur, L.F. Chibotaru, S. Gao, R. Sessoli, Chem. Eur. J. 19 (2013) 13726.

[9] (a) G. Cucinotta, M. Perfetti, J. Luzon, M. Etienne, P.E. Car, A. Caneschi, G. Calvez, K. Bernot, R. Sessoli, Angew. Chem., Int. Ed. 51 (2012) 16061610;
(b) J.D. Rinehart, J.R. Long, J. Am. Chem. Soc. 131 (2009) 1255812559;
(c) M.E. Boulon, G. Cucinotta, J. Luzon, C. Degl'Innocenti, M. Perfetti, K. Bernot, G. Calvez, A. Caneschi, R. Sessoli, Angew. Chem., Int. Ed. 52 (2013) 350354;
(d) E. Lucaccini, L. Sorace, M. Perfetti, J.P. Costes, R. Sessoli, Chem. Commun. 50 (2014) 16481651;
(e) J. Luzon, R. Sessoli, Dalton Trans. 41 (2012) 1355613567.

[10] (a) B.G. Wybourne, Spectroscopic Properties of Rare Earths, John Wiley and Sons, New York, 1965;
(b) A. Abragam, B. Bleaney, Electron Paramagnetic Resonance of Transition Ions, Oxford University Press, New York, 2012.

[11] (a) S. Stepanow, J. Honolka, P. Gambardella, L. Vitali, N. Abdurakhmanova, T.C. Tseng, S. Rauschenbach, S.L. Tait, V. Sessi, S. Klyatskaya, M. Ruben, K. Kern, J. Am. Chem. Soc. 132 (2010) 1190011901;
(b) S. Kyatskaya, J.R.G. Mascarós, L. Bogani, F. Hennrich, M. Kappes, W. Wernsdorfer, M. Ruben, J. Am. Chem. Soc. 131 (2009) 1514315151;
(c) A. Hofmann, Z. Salman, M. Mannini, A. Amato, L. Malavolti, E. Morenzoni, T. Prokscha, R. Sessoli, A. Suter, ACS Nano 6 (2012) 83908396;
(d) L. Margheriti, D. Chiappe, M. Mannini, P.E. Car, P. Sainctavit, M.A. Arrio, F.B. de Mongeot, J.C. Cezar, F.M. Piras, A. Magnani, E. Otero, A. Caneschi, R. Sessoli, Adv. Mater. 22 (2010) 54885493.

[12] (a) N. Ishikawa, M. Sugita, T. Ishikawa, S.Y. Koshihara, Y. Kaizu, J. Phys. Chem. B 108 (2004) 1126511271;
(b) S.D. Jiang, B.W. Wang, G. Su, Z.M. Wang, S. Gao, Angew. Chem., Int. Ed. 49 (2010) 74487451;
(c) G.J. Chen, Y.N. Guo, J.L. Tian, J. Tang, W. Gu, X. Liu, S.P. Yan, P. Cheng, D.Z. Liao, Chem. Eur. J. 18 (2012) 24842487;
(d) A. Yamashita, A. Watanabe, S. Akine, T. Nabeshima, M. Nakano, T. Yamamura, T. Kajiwara, Angew. Chem., Int. Ed. 50 (2011) 40164019;
(e) H.L.C. Feltham, Y. Lan, F. Klöer, L. Ungur, L.F. Chibotaru, A.K. Powell, S. Brooker, Chem. Eur. J. 17 (2011) 43624365;
(f) N. Ishikawa, Y. Mizuno, S. Takamatsu, T. Ishikawa, S. Koshihara, Inorg. Chem. 47 (2008) 1021710219;
(g) F. Branzoli, P. Carretta, M. Filibian, G. Zoppellaro, M.J. Graf, J.R. Galan-Mascaros, O. Fuhr, S. Brink, M. Ruben, J. Am. Chem. Soc. 31 (2009) 43874396;
(h) P.H. Lin, T.J. Burchell, R. Clérac, M. Murugesu, Angew. Chem., Int. Ed. 47 (2008) 88488851.

[13] (a) F. Pointillart, S. Klementieva, V. Kuropatov, Y. Le Gal, S. Golhen, O. Cador, V. Cherkasov, L. Ouahab, Chem. Commun. 48 (2012) 714716;
(b) J.K. Tang, I. Hewitt, N.T. Madhu, G. Chastanet, W. Wernsdorfer, C.E. Anson, C. Benelli, R. Sessoli, A.K. Powell, Angew. Chem., Int. Ed. 45 (2006) 17291733;
(c) M.T. Gamer, Y. Lan, P.W. Roesky, A.K. Powell, R. Clérac, Inorg. Chem. 47 (2008) 65816583.

[14] A. Bencini, C. Benelli, A. Caneschi, R.L. Carlin, A. Dei, D. Gatteschi, J. Am. Chem. Soc. 107 (1985) 81288136.

[15] (a) C.M. Zaleski, E.C. Depperman, J.W. Kampf, M.L. Kirk, V. Pecoraro, Angew. Chem., Int. Ed. 43 (2004) 39123914;
(b) F. Mori, T. Nyui, T. Ishida, T. Nogami, K.-Y. Choi, H. Nojiri, J. Am. Chem. Soc. 128 (2006) 14401441;
(c) M. Ferbinteanu, T. Kajiwara, K.Y. Choi, H. Nojiri, A. Nakamoto, N. Kojima, F. Cimpoesu, Y. Fujimura, S. Takaishi, M. Yamashita, J. Am. Chem. Soc. 128 (2006) 90089009;
(d) J.P. Costes, M. Auchel, F. Dahan, V. Peyrou, S. Shova, W. Wernsdorfer, Inorg. Chem. 45 (2006) 19241934;
(e) T.C. Stamatatos, S.J. Teat, W. Wernsdorfer, G. Christou, Angew. Chem., Int. Ed. 48 (2009) 521524;
(f) C.E. Burrow, T.J. Burchell, P.H. Lin, F. Habib, W. Wernsdorfer, R. Clérac, M. Murugesu, Inorg. Chem. 48 (2009) 80518053.

[16] (a) S. Osa, T. Kido, N. Matsumoto, N. Re, A. Pochaba, J. Mronzinski, J. Am. Chem. Soc. 126 (2004) 420;
(b) J.P. Costes, F. Dahan, W. Wernsdorfer, Inorg. Chem. 45 (2006) 5;
(c) T. Hamamatsu, K. Yabe, M. Towatari, N. Matsumoto, N. Re, A. Pochaba, J. Mrozinski, Bull. Chem. Soc. Jpn. 80 (2007) 523;
(d) T. Hamamatsu, K. Yabe, M. Towatari, S. Osa, N. Matsumoto, N. Re, A. Pochaba, J. Mrozinski, J.L. Gallani, A. Barla, P. Imperia, C. Paulsen, J.P. Kappler, Inorg. Chem. 46 (2007) 4458;
(e) Y.Q. Sun, M. Liang, W. Dong, G.M. Yang, D.Z. Liao, Z.H. Jiang, S.P. Yan, P. Cheng, Eur. J. Inorg. Chem. 7 (2004) 1514;
(f) C. Aronica, G. Pilet, G. Chastanet, W. Wernsdorfer, J.F. Jacquot, D. Luneau, Angew. Chem., Int. Ed. 45 (2006) 4659.

[17] (a) T. Yamaguchi, Y. Sunatsuki, H. Ishida, M. Kojima, H. Akashi, N. Re, N. Matsumoto, A. Pochaba, J. Mrozinski, Inorg. Chem. 47 (2008) 5736;
(b) T.D. Pasatoiu, M. Etienne, A.M. Madalan, M. Andruh, R. Sessoli, Dalton Trans. 39 (2010) 4802;
(c) J.P. Costes, T. Yamaguchi, M. Kojima, L. Vendier, Inorg. Chem. 48 (2009) 5555;
(d) R. Koner, H.H. Lin, H.H. Wei, S. Mohanta, Inorg. Chem. 44 (2005) 3524;
(e) T.D. Pasatoiu, J.P. Sutter, A.M. Madalan, F.Z.C. Fellah, C. Duhayon, M. Andruh, Inorg. Chem. 50 (2011) 58905898;
(f) E. Colacio, J. Ruiz-Sanchez, F.J. White, E.K. Brechin, Inorg. Chem. 50 (2011) 7268;
(g) K.C. Mondal, G.E. Kostakis, Y. Lan, W. Wernsdorfer, C.E. Anson, A.K. Powell, Inorg. Chem. 50 (2011) 11604;
(h) A. Okazawa, H. Nojiri, T. Ishida, N. Kojima, Polyhedron 30 (2011) 3140;
(i) S. Sakamoto, T. Fujinami, K. Nishi, N. Matsumoto, N. Mochida, T. Ishida, Y. Sunatsuki, N. Re, Inorg. Chem. 52 (2013) 7218.

[18] (a) V. Chandrasekhar, B.M. Pandian, R. Azhakar, J.J. Vittal, R.J. Clérac, Inorg. Chem. 46 (2007) 5140;
(b) T. Yamaguchi, J.P. Costes, Y. Kishima, M. Kojima, Y. Sunatsuki, N. Bruéfuel, J.P. Tuchagues, L. Vendier, W. Wernsdorfer, Inorg. Chem. 49 (2010) 9125;
(c) J.P. Costes, L. Vendier, W. Wernsdorfer, Dalton Trans. 40 (2011) 1700.

[19] (a) A. Mishra, W. Wernsdorfer, K.A. Abboud, G.J. Christou, J. Am. Chem. Soc. 126 (2004) 15648;
(b) J.L. Liu, F.S. Guo, Z.S. Meng, Y.Z. Zheng, J.D. Leng, M.L. Tong, L. Ungur, L.F. Chibotaru, K.J. Heroux, D.N. Hendrickson, Chem. Sci. 2 (2011) 1268.

[20] J. Long, R. Vallat, R.A.S. Ferreira, L.D. Carlos, F.A. Almeida Paz, Y. Guari, J. Larionova Chem. Commun. 48 (2012) 9974;
(b) T. Ishida, R. Watanabe, K. Fujiwara, A. Okazawa, N. Kojima, G. Tanaka, S. Yoshii, H. Nojiri, Dalton Trans. 41 (2012) 13609;
(c) M. Towatari, K. Nishi, T. Fujinami, N. Matsumoto, Y. Sunatsuki, M. Kojima, N. Mochida, T. Ishida, N. Re, J. Mrozinski, Inorg. Chem. 52 (2013) 6160.

[21] (a) T. Kajiwara, M. Nakano, S. Takaishi, M. Yamashita, Inorg. Chem. 47 (2008) 8604;
(b) T. Kajiwara, M. Nakano, K. Takahashi, S. Takaishi, M. Yamashita, Chem. Eur. J. 17 (2011) 196.

[22] (a) E. Coronado, J.R. Galán-Mascarós, C.J. Gómez-García, J.M. Martinez-Agudo, Inorg. Chem. 40 (2001) 113;
(b) M. Minguet, D. Luneau, E. Lhotel, V. Villar, C. Paulsen, D.B. Amabilino, J. Veciana, Angew. Chem., Int. Ed. 41 (2002) 586;
(c) E. Coronado, J.R. Galán-Mascarós, C.J. Gómez-García, A. Murcia-Martínez, Chem. Eur. J. 12 (2006) 3484;
(d) C. Train, R. Gheorghe, V. Krstic, L.M. Chamoreau, N.S. Ovanesyan, G.L.J.A. Rikken, M. Gruselle, M. Verdaguer, Nat. Mater. 7 (2008) 729.

[23] (a) A. Jana, S. Majumder, L. Carrella, M. Nayak, T. Weyhermueller, S. Dutta, D. Schollmeyer, E. Rentschler, R. Koner, S. Mohanta, Inorg. Chem. 49 (2010) 9012; (b) R. Koner, G.H. Lee, Y. Wang, H.H. Wei, S. Mohanta, Eur. J. Inorg. Chem. (2005) 1500.

[24] G.M. Sheldrick, SHELXL97, Program for Crystal Structure Refinement, University of Göttingen, Göttingen, Germany, 1997.

[25] Y. Wang, X.L. Li, T.W. Wang, Y. Song, X.Z. You, Inorg. Chem. 49 (2010) 969976.

[26] J. Dreiser, K.S. Pedersen, C. Piamonteze, S. Rusponi, Z. Salman, Md.E. Ali, M. Schau-Magnussen, C.A. Thuesen, S. Piligkos, H. Weihe, H. Mutka, O. Waldmann, P. Oppeneer, J. Bendix, F. Nolting, H. Brune, Chem. Sci. 3 (2012) 10241032.

[27] L. Zhao, J. Wu, H. Ke, J. Tang, Inorg. Chem. 53 (2014) 35193525.

[28] S.J. Liu, J.P. Zhao, W.C. Song, S.D. Han, Z.Y. Liu, X.H. Bu, Inorg. Chem. 52 (2013) 21032109.

[29] (a) J. Ruiz, A.J. Mota, A. Rodríguez-Diéguez, S. Titos, J.M. Herrera, E. Ruiz, E. Cremades, J.P. Costes, E. Colacio, Chem. Commun. 48 (2012) 79167918; (b) C.M. Liu, D.Q. Zhang, D.B. Zhu, Inorg. Chem. 52 (2013) 89338940.

[30] (a) Y.-N. Guo, G.-F. Xu, P. Gamez, L. Zhao, S.-Y. Lin, R. Deng, J. Tang, H.-J. Zhang, J. Am. Chem. Soc. 132 (2010) 8538; (b) C.M. Liu, D.Q. Zhang, X. Hao, D.B. Zhu, Chem. Asian J. 9 (2014) 1847.

[31] V. Chandrasekhar, P. Bag, W. Kroener, K. Gieb, P. Müller, Inorg. Chem. 52 (2013) 13078.